

Technical University of Denmark



Establishing exchange bias below T-N with polycrystalline Ni_{0.52}Co_{0.48}O/Co bilayers

Berkowitz, A.E.; Hansen, Mikkel Foug; Tang, Y.J.; Hong, Y.I.; Smith, D.J.

Published in:
Physical Review B (Condensed Matter and Materials Physics)

Link to article, DOI:
[10.1103/PhysRevB.72.134428](https://doi.org/10.1103/PhysRevB.72.134428)

Publication date:
2005

Document Version
Publisher's PDF, also known as Version of record

[Link back to DTU Orbit](#)

Citation (APA):
Berkowitz, A. E., Hansen, M. F., Tang, Y. J., Hong, Y. I., & Smith, D. J. (2005). Establishing exchange bias below T-N with polycrystalline Ni_{0.52}Co_{0.48}O/Co bilayers. *Physical Review B (Condensed Matter and Materials Physics)*, 72(13), 134428. DOI: 10.1103/PhysRevB.72.134428

DTU Library

Technical Information Center of Denmark

General rights

Copyright and moral rights for the publications made accessible in the public portal are retained by the authors and/or other copyright owners and it is a condition of accessing publications that users recognise and abide by the legal requirements associated with these rights.

- Users may download and print one copy of any publication from the public portal for the purpose of private study or research.
- You may not further distribute the material or use it for any profit-making activity or commercial gain
- You may freely distribute the URL identifying the publication in the public portal

If you believe that this document breaches copyright please contact us providing details, and we will remove access to the work immediately and investigate your claim.

Establishing exchange bias below T_N with polycrystalline $\text{Ni}_{0.52}\text{Co}_{0.48}\text{O}/\text{Co}$ bilayers

A. E. Berkowitz

Department of Physics and Center for Magnetic Recording Research, University of California at San Diego,
La Jolla, California 92093-0401, USA

M. F. Hansen

MIC—Department of Micro and Nanotechnology, Technical University of Denmark, DK-2800 Kongens Lyngby, Denmark

R. H. Kodama

Department of Physics, University of Illinois at Chicago, Chicago, Illinois 60607-7059, USA

Y. J. Tang and J. I. Hong

Center for Magnetic Recording Research, University of California at San Diego, La Jolla, California 92093-0401, USA

David J. Smith

Department of Physics and Astronomy and Center for Solid State Science, Arizona State University, Tempe, Arizona 85287-1504, USA

(Received 16 August 2005; revised manuscript received 7 September 2005; published 31 October 2005)

Exchange-coupled bilayers of polycrystalline ferromagnetic (FM) Co on antiferromagnetic (AFM) $\text{Ni}_{0.52}\text{Co}_{0.48}\text{O}$ were investigated with emphasis on the issue of establishing an exchange-bias field, H_E , below the AFM ordering temperature, T_N . It was found that field-cooling the bilayers through T_N provided very little, if any, increase in H_E over that produced by deposition of the Co at temperatures far below T_N . Further significant aspects of this issue were also examined. The biasing field, H_B , needed to be applied only during the deposition of a small fraction (1 nm) of the FM film below T_N of the AFM to achieve the maximum H_E ; if H_B was reversed at any time during the FM deposition, H_E was determined by the final direction of H_B ; the direction of H_E could be reversed after it had been established by applying a reversed field during a post-deposition latent period. These and other findings are considered with respect to clarification of the mechanisms for establishing H_E .

DOI: 10.1103/PhysRevB.72.134428

PACS number(s): 75.70.Cn, 75.75.+a

INTRODUCTION

Meiklejohn and Bean reported their discovery of exchange anisotropy^{1,2} in systems of Co nanoparticles with an antiferromagnetic (AFM) CoO surface layer. More recently, bilayer studies using well-characterized polycrystalline CoO films, have yielded a quantitatively predictive model for the exchange-bias-field, H_E , emphasizing the origin and predominant role of uncompensated AFM spins.³ A basic premise of this model, the dependence of the uncompensated AFM spin density on the interfacial AFM grain size, has been confirmed by work with $\text{Co}_{0.5}\text{Ni}_{0.5}\text{O}$ films.⁴ Since the ordering temperature, T_N , of CoO is 293 K, experiments using this system involve field-cooling the samples through T_N to produce the exchange bias. However, it is well recognized, and extensively employed in the fabrication of sensors for computer hard disks, that it is only necessary to deposit the ferromagnetic (FM) film on the AFM film in a biasing field to establish H_E , even if the deposition temperature is below T_N of the AFM. This provocative feature of exchange anisotropy has not received much attention, aside from the investigation of Tong *et al.*⁵ These authors investigated trilayer structures consisting of CoFe films sandwiching an IrMn film. The thicknesses of the CoFe films ranged from 2.0 to 5.0 nm, and the IrMn thicknesses were from 2.0 to 7.0 nm. It was found that even when the CoFe and IrMn films were each only of the order of one grain thick, H_E

of the upper CoFe film could be set in arbitrary directions with respect to the preset direction of H_E of the lower CoFe film. The direction of H_E for the top CoFe film depended only on the direction of the bias field applied during its deposition. Deposition was carried out at ambient temperature, below the blocking temperature, $T_B=225$ °C.

The very small thickness of the IrMn films makes it unlikely that domain walls parallel to the interface⁶ exist in the AFM. This result led Tong *et al.* to suggest that in their polycrystalline AFM films, exchange interactions with some grains could accommodate the upper H_E orientation, whereas others could favor the lower H_E direction, although the details were unclear.

When field-cooling an FM-AFM bilayer through T_N or T_B , the usual mechanism invoked is that, on passing through the very low anisotropy region near T_N or T_B , the AF grains choose from their equivalent spin distributions the one most favorable for coupling to the FM.^{1,2} Equivalently, in view of the low anisotropy of the AFM near T_N , the polarized FM which is exchange coupled to the uncompensated interfacial AFM spins, can reverse the Néel axes of interfacial grains so that their associated uncompensated spins have a component along the polarization direction.³ These considerations suggest that H_E would be much greater for an FM-AFM bilayer field-cooled through T_B than if the FM film were deposited on top of an AFM film in a field below T_B , since more AFM grains with randomly oriented Néel axes would have favor-

ably oriented spin configurations in the former case. In the present study using the AFM monoxide $\text{Ni}_{0.52}\text{Co}_{0.48}\text{O}$, we find that this prediction of the orthodox theory is false. We also have investigated the related issue of whether substrate heating during the deposition process can be responsible for our results.

EXPERIMENTAL APPROACH

In order to conveniently investigate the H_E behavior when the FM film was deposited in a bias-field, H_B , below T_N of the AFM film, we used $\text{Ni}_{0.52}\text{Co}_{0.48}\text{O}$, with $T_N=144^\circ\text{C}$, for the AFM, and Co for the FM. The dependence of H_E on an extensive range of deposition conditions was investigated. These are listed below with identifying tags to facilitate reference to specific experiments described later in the paper. All samples had a capping layer of ≥ 5 nm rf-sputtered SiO_2 .

(a) 25 nm of Co was deposited in $H_B=0$ at RT on 50 nm of $\text{Ni}_{0.52}\text{Co}_{0.48}\text{O}$, and the bilayer was then cooled in $H_B \approx 100$ Oe from several temperatures $T \leq 150^\circ\text{C}$, to RT.

(b) Bilayers with 25, 15, and 10 nm of Co were deposited at 77 K and at RT on 50 nm of $\text{Ni}_{0.52}\text{Co}_{0.48}\text{O}$ in H_B and the resulting RT H_E and training behavior were compared. The 25 and 15 nm samples deposited at both temperatures were also cooled from 150°C in H_B , and their RT H_E and training behavior determined.

(c) With 25 nm of Co deposited at RT on 50 nm of $\text{Ni}_{0.52}\text{Co}_{0.48}\text{O}$.

(1) $H_B \approx 100$ Oe was applied only during selected initial and final portions of the Co deposition.

(2) The direction of H_B was changed during selected initial and final portions of the Co deposition.

(3) The direction of H_B was changed ≈ 15 min after deposition of the 5 nm SiO_2 capping layer.

(4) An additional 30 nm of SiO_2 was deposited on a three-month-old sample with H_B antiparallel to the original direction.

SAMPLE PREPARATION

The three film layers— $\text{Ni}_{0.52}\text{Co}_{0.48}\text{O}$, Co, SiO_2 cap—were always deposited in that order during a single pump-down. The films were sputtered in a chamber with a background pressure of $\sim 2 \times 10^{-7}$ torr. Substrates were (100) Si wafers with native oxide. These were mounted and thermally clamped in Cu holders on a table rotating above the sputtering targets. The substrate table could be cooled to 77 K. $H_B \approx 100$ Oe was provided by a permanent magnet array backing the substrates. An *in situ* mask changer was used to move substrates from holders with a backing magnet to holders without a backing magnet. This feature was used for all experiments listed under (c) with the substrates shielded with shutters from the sputtered flux during the position changes which took about 30 s. After a deposition and before changing conditions (e.g., H_B , stopping rotation of sputtering table, or venting oxygen), a 15 min pause was observed to ensure thermal equilibrium. The 77 K and RT depositions of each Co thickness listed under (b) were both made in the same

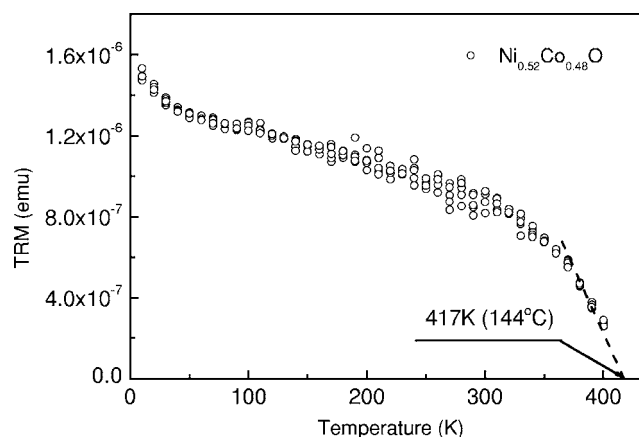


FIG. 1. Thermoremanent magnetization (TRM) of 50 nm $\text{Ni}_{0.52}\text{Co}_{0.48}\text{O}$ film after cooling in 2.5 T from 400 K and warming in $H=0$.

pump-down on $\text{Ni}_{0.52}\text{Co}_{0.48}\text{O}$ films deposited simultaneously at RT in that same pump-down.

The $\text{Ni}_{0.52}\text{Co}_{0.48}\text{O}$ films were reactively dc magnetron sputtered from nominal $\text{Ni}_{0.5}\text{Co}_{0.5}$ targets in a pressure of ≈ 2 mTorr Ar with a partial pressure of oxygen (Ar flow: 30 sccm; O flow: 2 sccm). The deposition rate was ≈ 1.9 nm/min. The Co films were dc magnetron sputtered in a pressure of 2 mTorr Ar (ar flow: 30 sccm) at a deposition rate of ≈ 1.2 nm/min.

CHARACTERIZATION

X-ray diffraction (XRD) spectra were obtained on a Rigaku D/max-B system with Co radiation. Transmission electron micrographs (TEM) of sample cross sections were recorded with a JEOL 4000EX high-resolution electron microscope operated at 400 keV. Magnetic properties were measured with an alternating gradient magnetometer (AGM) or vibrating sample magnetometer (VSM) at room temperature in maximum fields between 3 kOe and 10 kOe; low temperature measurements were made in a SQUID magnetometer. The thermal treatments indicated in (b) were made in vacuum of $\sim 10^{-7}$ Torr. The thermal treatments noted in (a) were made in the VSM in a flowing Ar atmosphere.

EXPERIMENTAL RESULTS

Composition and structure

A film of 50 nm of Ni—Co—O was deposited from the nominal $\text{Ni}_{0.50}\text{Co}_{0.50}$ target in the standard manner on a Si wafer without any Co or SiO_2 cap in order to determine its composition and T_N . A number of EDX measurements gave an average cation ratio of 52 Ni/48 Co ± 1 atom%. To determine T_N , the thermoremanent magnetization (TRM) of the same film was measured in zero field on warming in a SQUID magnetometer after cooling in 2.5 T from 400 K. The signal was that of the uncompensated spins of the $\text{Ni}_{0.52}\text{Co}_{0.48}\text{O}$ which were put in a remanent state after field-cooling through a temperature region of very low anisotropy. Figure 1 shows the TRM data. The TRM vanishes by ex-

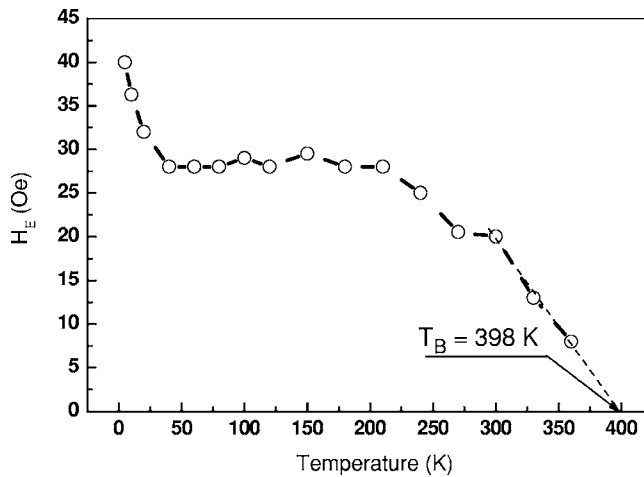


FIG. 2. Temperature dependence of H_E of $\text{Ni}_{0.52}\text{Co}_{0.48}\text{O}(50 \text{ nm})/\text{Co}(25 \text{ nm})/\text{SiO}_2(5 \text{ nm})$ after field cooling from 400 K to 5 K in 10 kOe.

trapolation at 417 K (144 °C), which we consider to be T_N , since this value is in excellent agreement with the published value for the measured composition.⁷

Figure 2 shows the temperature dependence of H_E after field-cooling from 400 K to 5 K in 10 kOe. T_B is 398 K, as obtained by extrapolation. The $H_E(T)$ dependence is qualitatively the same as found for Co/CoO ,³ however, the relatively flat region extends down to ≈ 40 K, as compared to ≈ 50 K for CoO , and the upswing at lower temperatures is stronger and sharper.

XRD spectra of two samples prepared for (b), with Co sputtered at RT and 77 K on $\text{Ni}_{0.52}\text{Co}_{0.48}\text{O}$ which was deposited at RT are shown in Fig. 3. The sample plane was rotated a few degrees to eliminate the strong peak from the Si substrate. Both the Co and $\text{Ni}_{0.52}\text{Co}_{0.48}\text{O}$ films show (111) texture. There is no difference between the samples deposited at RT and 77 K. The Co (111) peak indicates an fcc Co structure with a lattice parameter of $a_0 = 3.535 \text{ \AA}$. Fitting of the $\text{Ni}_{0.52}\text{Co}_{0.48}\text{O}$ (111) and (220) peaks gave a lattice parameter

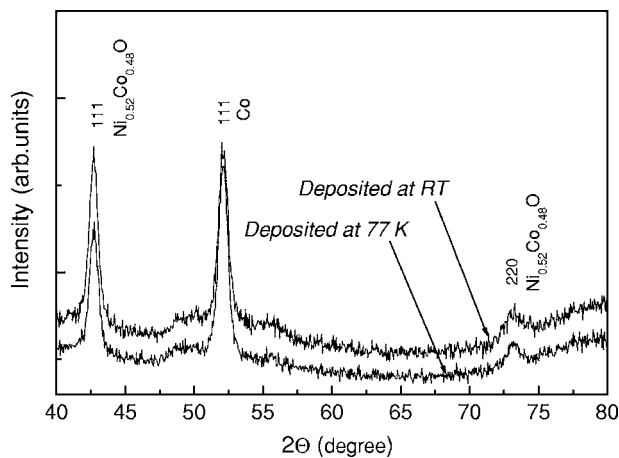


FIG. 3. X-ray diffraction spectra of $\text{Ni}_{0.52}\text{Co}_{0.48}\text{O}(50 \text{ nm})/\text{Co}(25 \text{ nm})/\text{SiO}_2(5 \text{ nm})$ deposited at room temperature and 77 K. Si substrate tilted to minimize the (100) peak from the Si substrate.

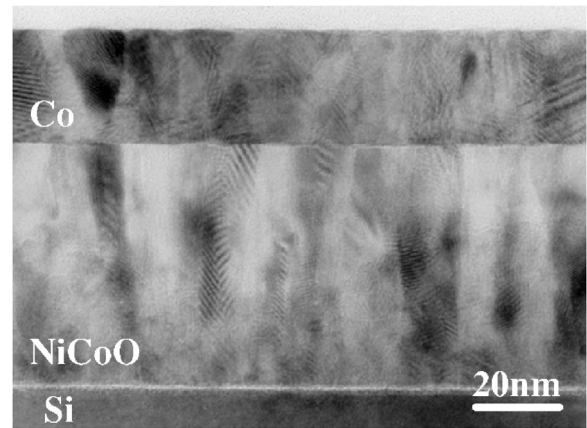


FIG. 4. TEM micrograph of $\text{Ni}_{0.52}\text{Co}_{0.48}\text{O}(50 \text{ nm})/\text{Co}(25 \text{ nm})/\text{SiO}_2(7.5 \text{ nm})$ on a (100) Si wafer with its native oxide.

of $a_0 = 4.246 \pm 0.006 \text{ \AA}$ for a simple cubic structure, intermediate between those of NiO ($a_0 = 4.177 \text{ \AA}$) and CoO ($a_0 = 4.260 \text{ \AA}$).

A TEM micrograph of a typical trilayer of $\text{Ni}_{0.52}\text{Co}_{0.48}\text{O}(50 \text{ nm})/\text{Co}(25 \text{ nm})/\text{SiO}_2(7.5 \text{ nm})$ on a (100) Si wafer with native oxide is shown in Fig. 4. The grain sizes of the $\text{Ni}_{0.52}\text{Co}_{0.48}\text{O}$ and the Co at their very sharp interface are both $\approx 10 \text{ nm}$, with no evidence of epitaxy. This microstructure led us to assume that each $\approx 10 \text{ nm}$ AFM interfacial crystallite is a single AFM domain, since it is energetically unlikely that domain walls could be present in such small regions.

Magnetic

(a) Cooling in $H_B \approx 100 \text{ Oe}$ from $T \leq 150 \text{ }^\circ\text{C}$

As noted above, there is a question as to whether the effective deposition temperature is high enough above the nominal ambient RT to provide for field-cooling (FC) in $H_B \approx 100 \text{ Oe}$ to reverse the Néel axes of some AFM interfacial grains such that their associated uncompensated spins have a component in the direction of the FM magnetization. Thus it was pertinent to determine the dependence of H_E on the starting temperature for field-cooling. Figure 5(a) shows easy and hard axis hysteresis loops with Co deposited at RT in H_B . Figures 5(b), 5(c), and 5(d), are loops for films in which 25 nm of Co was deposited in $H_B = 0$ at RT on 50 nm of $\text{Ni}_{0.52}\text{Co}_{0.48}\text{O}$, and then the bilayers were cooled in $H_B \approx 100 \text{ Oe}$ from temperatures, $T = 50, 75,$ and $150 \text{ }^\circ\text{C}$, respectively. H_E is $\approx 10\%$ higher for the Co film deposited at RT than for the one cooled from $150 \text{ }^\circ\text{C}$, and much higher than H_E for the bilayers cooled from lower temperatures.

(b) Comparing RT and 77 K depositions

As an additional test of the significance of the nominal deposition temperature, bilayers with 25, 15, and 10 nm of Co were deposited in $H_B \approx 100 \text{ Oe}$ at 77 K and at RT on 50 nm of $\text{Ni}_{0.52}\text{Co}_{0.48}\text{O}$ which was sputtered at RT. A 5 nm SiO_2 capping layer was applied to all samples. Each of these

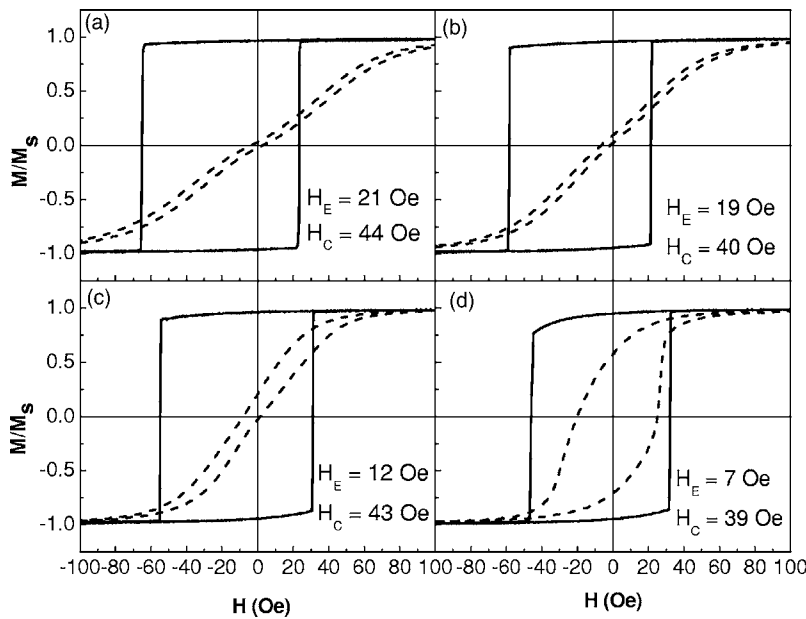


FIG. 5. Easy axis (solid) and hard axis (dashed) hysteresis loops measured at room temperature on $\text{Ni}_{0.52}\text{Co}_{0.48}\text{O}$ (50 nm)/Co (25 nm)/ SiO_2 (5 nm). (a) Co deposited at room temperature in $H_B \approx 100$ Oe. In (b), (c), and (d), 25 nm of Co was deposited in $H_E = 0$, and then the samples were cooled in H_B from temperatures, $T = 150, 75,$ and 50°C , respectively.

film samples was grown in a single pump-down. In addition, the 25 and 15 nm samples deposited at both temperatures were also cooled from 150°C in H_B .

25 nm Co. Figure 6 shows the hysteresis loops for the 25 nm Co samples deposited at RT and 77 K in H_B , and after cooling in $H_B \approx 100$ Oe from 150°C . H_E differed by < 1 Oe for the as-prepared samples deposited at both temperatures. After FC from 150°C , the samples had virtually identical H_E , which was about 1 Oe higher than the as-prepared values. There was no training for either sample, as-deposited or field-cooled. The coercive force (H_C) increased by ≈ 1 Oe for each sample after FC, and the values were ≈ 3 Oe higher for the samples prepared at 77 K. Thus, for the 25 nm Co samples deposition at RT or 77 K made very little difference in H_E , either before or after FC. H_C was about 10% higher

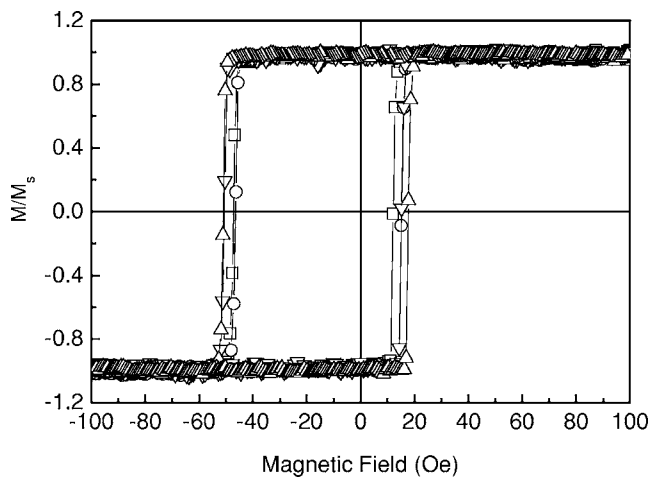


FIG. 6. Hysteresis loops of $\text{Ni}_{0.52}\text{Co}_{0.48}\text{O}$ (50 nm)/Co (25 nm)/ SiO_2 (5 nm) measured at room temperature after deposition of entire sample at room temperature (RT) and 77 K in $H_B \approx 100$ Oe. (O), deposited at RT; (square), deposited at RT, cooled in H_B from 150°C ; (triangle), deposited at 77 K; (inverted triangle), deposited at 77 K, cooled in $H_B \approx 100$ Oe from 150°C .

for the films deposited at 77 K; FC made no significant change in H_C for either sample.

15 nm Co. Figure 7 shows the trend of H_E and H_C for both samples, before and after FC, as functions of the number of field cycles. Both as-prepared samples exhibited training in H_E , but H_C was essentially constant (< 1 Oe decrease). After FC, there was negligible evidence of training. H_E was ≈ 2 Oe higher for the 77 K sample, as-prepared and trained, and ≈ 1 Oe higher after FC. H_C was 2–3 Oe higher for the 77 K sample, as-prepared. After FC, H_C was the same for both samples.

10 nm Co. Figure 8 summarizes H_E and H_C for both deposition temperatures as functions of field cycles. Since H_C of the 77 K sample was so close to the ≈ 100 Oe field of H_B , these samples were not field-cooled. H_E is larger for the 77 K sample, in contrast to the case for the 25 and 15 nm samples. H_C is constant for both samples, but is much larger for the 77 K sample. The training behavior of these samples

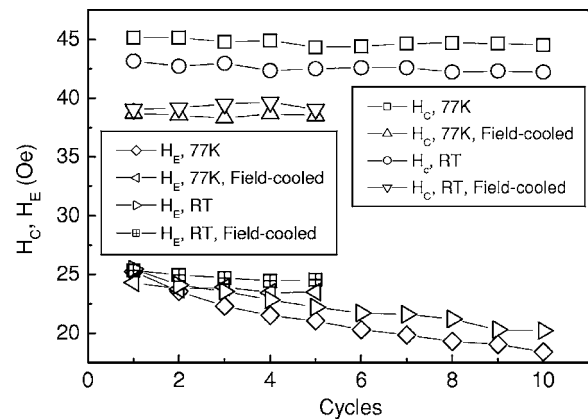


FIG. 7. H_E and H_C of $\text{Ni}_{0.52}\text{Co}_{0.48}\text{O}$ (50 nm)/Co (15 nm)/ SiO_2 (5 nm) measured at room temperature, as functions of number of field cycles, after deposition of the entire sample at room temperature (RT) and 77 K in $H_B \approx 100$ Oe. Shown are values for as-deposited samples, and after field cooling in H_B from 150°C .

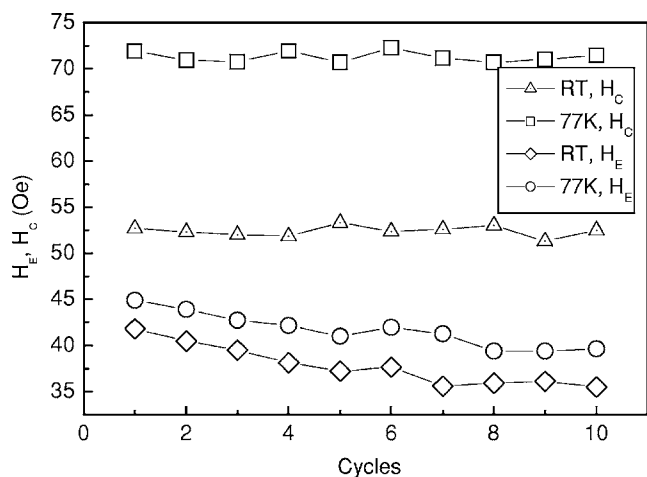


FIG. 8. H_E and H_C of $\text{Ni}_{0.52}\text{Co}_{0.48}\text{O}$ (50 nm)/Co (10 nm)/ SiO_2 (5 nm) measured at room temperature, as functions of number of field cycles, after deposition of entire sample at room temperature (RT) and 77 K in $H_B \approx 100$ Oe.

also differs from that of the thicker samples. There is significant training for the first few cycles, but a relatively stable H_E thereafter.

It is noteworthy that all hysteresis loops for these samples, including the ones cycled for training measurement, are as square as those shown in Fig. 6. Moreover, differences of 1 or 2 Oe in H_E and H_C are not significant in view of sample thickness and magnetic measurement uncertainties.

(c-1) H_B applied during portions of initial and final Co deposition

Pairs of samples with inverse deposition conditions were prepared in the same run in the following manner. Two substrates were placed in diametrically opposite sample holders on the rotating substrate table. One was placed in a holder with a backing magnet; the other in a holder without a backing magnet. After 50 nm of $\text{Ni}_{0.52}\text{Co}_{0.48}\text{O}$ was simultaneously deposited on the substrates, a thickness, x , of the 25 nm of Co was deposited on them. The positions of the substrates were then switched with the mask changer, and the remainder of the 25 nm of Co was deposited. Thus, for each selected fraction of Co thickness, one substrate had H_B applied only during the initial step, and another sample had H_B applied only during the final step. Thus, a constant total Co thickness was maintained, but H_B was applied only during selected portions of the Co layer deposition.

Figure 9 shows the resulting hysteresis loops after depositing the initial part of the 25 nm Co layer in the applied field, $H_B \approx 100$ Oe, and the remainder (and SiO_2 capping layer) with $H_B = 0$. The hard direction hysteresis loop for $x = 1$ nm is typical for all the hard direction hysteresis loops. H_E is virtually constant for all thicknesses for which H_B was applied. Remarkably, H_B need be applied during only the initial 1 nm of Co to obtain the equilibrium value of H_E . H_C is constant for all of these samples.

The hysteresis loops from samples with opposite field conditions (i.e., no H_B during the initial part of the Co layer, but H_B applied during the final part of the Co layer) are shown in Fig. 10. For this protocol, very similar values of H_E

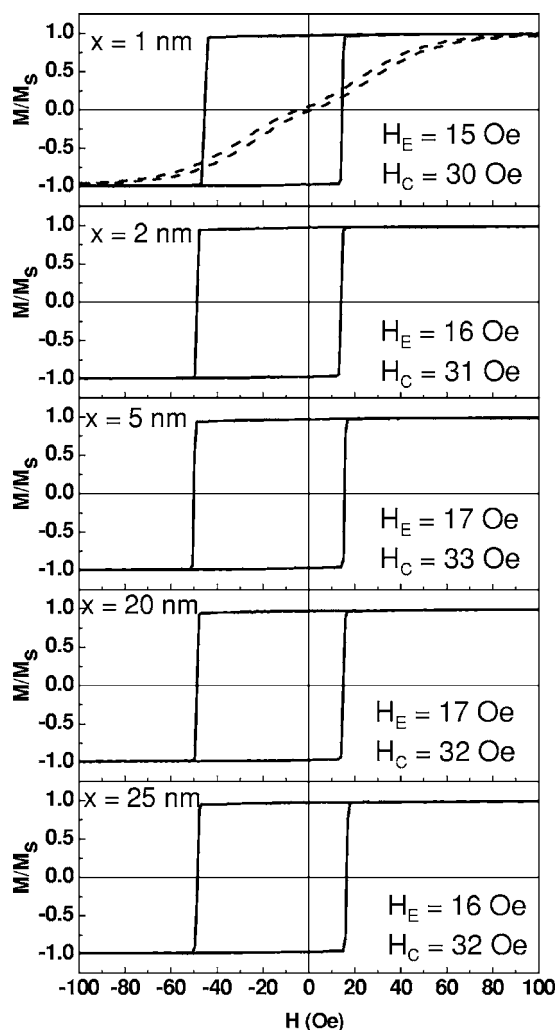


FIG. 9. Hysteresis loops of $\text{Ni}_{0.52}\text{Co}_{0.48}\text{O}$ (50 nm)/Co (25 nm)/ SiO_2 (5 nm) measured at room temperature after depositing the initial part (x nm) of the 25 nm Co layer in an applied field, H_B , and the remainder (and SiO_2 capping layer) with $H_B = 0$.

are again obtained for all choices of the thickness, x , for which H_B is applied. These H_E values are comparable to the H_E values in Fig. 9. Thus, the conclusion from these data sets is that H_B need be applied only during a small portion of the Co deposition, or even just during the deposition of the SiO_2 capping layer ($x = 25$ nm in Fig. 10), for the equilibrium H_E to be established below T_N .

(c-2) Changing direction of H_B during Co deposition

In these experiments, H_B was in the (+) or (-) direction during an initial portion of the Co deposition, then rotated to the (-) or (+) direction for the final portion. With H_B in the positive field direction, the hysteresis loop is shifted to negative fields, and *vice versa*. Figure 11 shows the hysteresis loops with H_B applied in the (+) or (-) directions for the first 5 and 20 nm, and then switched to the (-) or (+) directions for the final 20 and 5 nm, respectively. The data show that the direction of H_E depends only on the direction of H_B during the final portion of the Co deposition for anti-parallel directions of H_B .

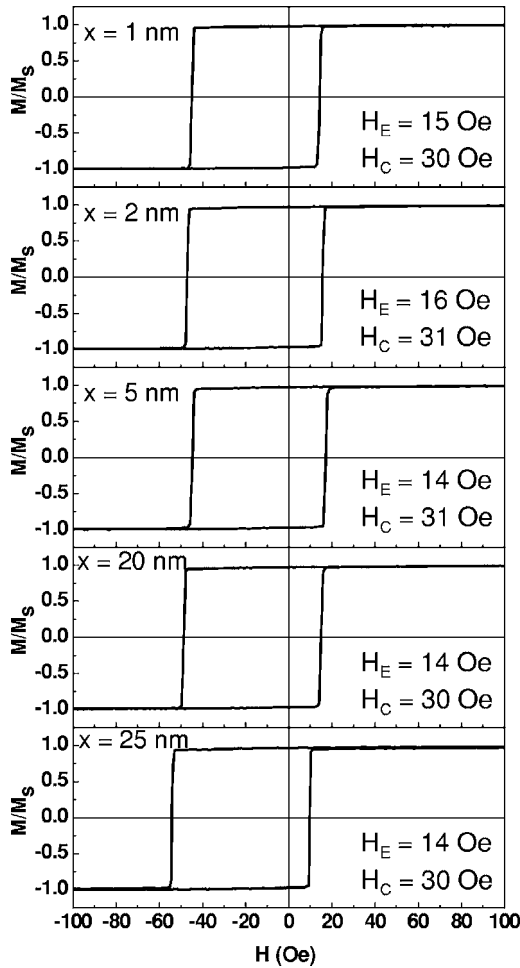


FIG. 10. Hysteresis loops of $\text{Ni}_{0.52}\text{Co}_{0.48}\text{O}$ (50nm)/Co(25 nm)/ SiO_2 (5 nm) measured at room temperature after depositing the initial part (x nm) of the 25 nm Co layer in $H=0$, and the remainder (and SiO_2 capping layer) with $H_B \approx 100$ Oe.

(c-3) Changing direction of H_B shortly after completing deposition

The complete trilayer— $\text{Ni}_{0.52}\text{Co}_{0.48}\text{O}$, Co, SiO_2 —was deposited in $(-)$ or $(+)$ H_B and remained in that condition for ≈ 15 min. Then the trilayer was held for 20 min with H_B reversed. Figure 12 shows the hysteresis loops for $(+)$ or $(-)$ final directions of H_B . The direction of H_E is set or changed by exposing the films to an antiparallel H_B a short time after the deposition, but with a significant reduction of $|H_E|$, as compared with previous samples.

(c-4) Deposition of additional SiO_2 with antiparallel H_B long after initial deposition

As an additional test of the possible heating effect of the deposition process, H_B was applied to a 3-month-old sample antiparallel to the initial direction while an additional 30 nm of SiO_2 was deposited. There was no change in H_E . Thus, there is a latent period during which most of H_E can be rotated by rotating H_B and holding for 20 min after depositing the trilayer and waiting ≈ 15 min, as well as by applying H_B only during the capping layer deposition. For a longer

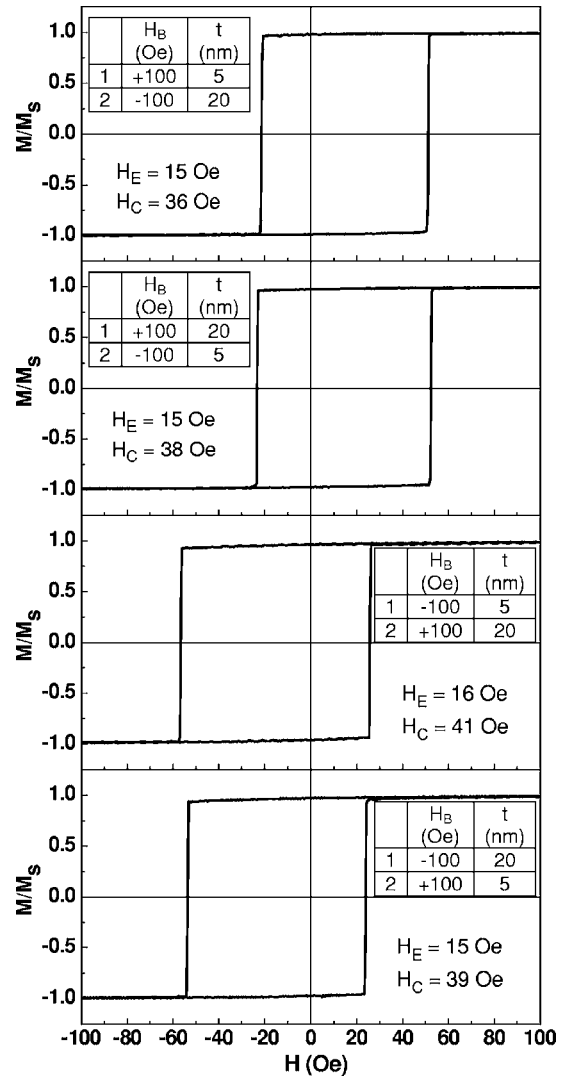


FIG. 11. Hysteresis loops of $\text{Ni}_{0.52}\text{Co}_{0.48}\text{O}$ (50 nm)/Co (25 nm)/ SiO_2 (5 nm) measured at room temperature. H_B was in the $(+)$ or $(-)$ direction during an initial (1) portion ($x=5, 20$ nm) of the Co deposition, then rotated to the $(-)$ or $(+)$ direction for the final (2) portion (20, 5 nm). The hysteresis loops correspond to the final bias field direction.

period—somewhere between 15 min and a few days (the minimum time between sample deposition and measurement for samples exhibiting no training)— H_E cannot be reversed, even with the energy supplied by depositing 30 nm of SiO_2 .

DISCUSSION

It seems appropriate to consider the impact of these results on two principal issues. One is the difference in the properties of the FM/AFM bilayers when field-cooled through T_N or when the FM layer is deposited at a temperature nominally below T_N . The second, much broader question, is what the results imply about the mechanism by which H_E is established in general, and below T_N in particular.

Probably the most surprising result is the existence of a “latent period” after deposition, lasting at least 15 min. and

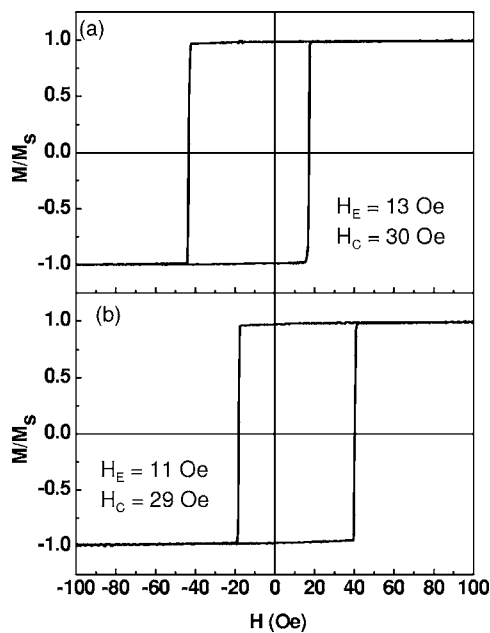


FIG. 12. Hysteresis loops of $\text{Ni}_{0.52}\text{Co}_{0.48}\text{O}$ (50 nm)/Co (25 nm)/ SiO_2 (5 nm) measured at room temperature. The films were deposited in (a) $H_B \approx -100$ Oe, and (b) $H_B \approx +100$ Oe. After the deposition, this field condition was maintained for 15 min, after which the sign of H_B was reversed and the sample was left in the reverse direction for 20 min. The hysteresis loops are those for the final directions of H_B .

as much as several days, during which the bias direction can be changed by application of a small field (e.g., 100 Oe). In the following, we will refer to later times as the “postlatent period,” during which the bias direction becomes frozen-in, requiring heating to near T_N (417 K/144 °C) to substantially modify its direction or strength. The physical origin of the latent period is unknown, but likely candidates are (1) interfacial redox reactions (discussed below), and (2) slow relaxation of the magnetic state.

The 25 nm Co samples deposited at both RT and 77 K (Fig. 6) show the same H_E values (within measurement uncertainties) for as-deposited and FC samples. They also exhibit no training. Thus, it appears that for an AFM-FM bilayer with a thick enough FM layer to exhibit no training, there is no significant difference in H_E between field-cooling from above T_N and depositing the FM layer at temperatures well below T_N . In the course of our investigation, these 77 K depositions were used to assess the possible role of sample heating during deposition. However, in light of the remarkable latent effects, the significance of this result is not so clear. Presumably when the samples are warmed to room temperature, they are still in the latent period, allowing H_E to further develop. Furthermore, the energetics of some of the interfacial redox reactions may allow them to occur at temperatures as low as 77 K. The data in Fig. 5 indicate that in the post-latent period, a temperature of ≈ 150 °C is required to establish the fully biased state. However, although H_E of the 15 nm Co RT and 77 K samples are virtually the same, as-deposited and immediately after FC (Fig. 7), training reduces the as-deposited values by $\approx 20\%$ after 10 field cycles,

whereas the FC samples show negligible training. It is notable that for both the 15 and 10 nm bilayers, H_C shows no training, in contrast to the H_E behavior. Several plausible assumptions could reconcile these different responses of H_C and H_E to field cycling, although a detailed theoretical treatment has yet to be done. It seems reasonable to assume that H_C is dependent on the pinning energies at inhomogeneities in the FM-AFM exchange. We assume that the orientations and magnitude of the uncompensated spins at pinning sites vary, with a corresponding variation of the localized FM-AFM exchange interactions. Field cycling may eliminate some localized coupling involving weakest exchange interactions, while leaving unaltered those pinned sites with strongest exchange interactions (and largest pinning energy). We suppose that H_C is related to the strongest pinning sites, but that all contribute to H_E . Sharp switching usually results from the nucleation of a reverse domain which sweeps across the FM film,⁸ but it may also reflect a relatively homogeneous distribution of such pinning sites, as compared to those arising from impurities or other structural defects. The pinning energy likely contributes to the magnitude of this nucleation field, but other properties of the FM film, such as film thickness, intrinsic magnetocrystalline anisotropy, and stress, also contribute.

The data in Fig. 9, showing that H_B need be applied only during deposition of the first nm ($x=1$ nm) of the 25 nm Co film, to achieve the full H_E , is not immediately obvious. The 1 nm Co film on $\text{Ni}_{0.52}\text{Co}_{0.48}\text{O}$ shows large H_E at RT, and requires approximately 1500 Oe to saturate.¹⁴ Therefore, the 100 Oe H_B is not sufficient to fully saturate the 1 nm Co film. The remarkability of the result is emphasized by the fact that TEM cross sections of a 1 nm Co film on a 50 nm $\text{Ni}_{0.52}\text{Co}_{0.48}\text{O}$ film capped with SiO_2 show that the Co film is not even continuous.¹⁴ However, as deposition continues and the film grows thicker, the results suggest that the film spontaneously saturates along the original H_B direction, even after the H_B is removed. This idea is also supported by the squareness of the loops for thicker Co films. Given these considerations and the latent effects described below, one can understand how the full H_E is developed, even for $x=1$ nm.

The data in Fig. 10 show the reverse— H_B need be applied only during the latter portion of the deposition of the Co, and the full H_B and H_C are obtained. This is the initial evidence for a latency property—that there is a time period during which H_E can be altered by changing the applied field. Figure 11 shows that H_E can be completely reversed by reversing H_B during deposition of the Co. Figure 12 is the most explicit demonstration of a latent period. Even 20 minutes after the deposition was completed and H_B applied for an additional 15 min, if a reverse H_B is applied, a major fraction of H_E is reversed. Alternatively, after this treatment, a minor fraction of H_E was stable against reversal. The kinetic processes implied by this latency behavior are quite consistent with the reactions and interactions that take place at the FM-AFM interface.

Redox reactions are present at the interfaces of exchange couples with AFM monoxides^{15,16} and involve diffusion of oxygen atoms. Defect-generated interfacial diffusion is likely to be present over several monolayers. Then there is the question of the nature of the bonding, chemical and mag-

netic, that couples the compensated AFM cations with FM atoms; these constitute the vast majority of interfacial species. Presently, the interfacial, atom-specific data needed to permit reliable models of these kinetic processes are not available.

Interfacial redox reactions are essentially a process of reforming the gross electronic state of the interface. Clearly, the more subtle (i.e., smaller energy scale), magnetic aspect of the electronic state of the interface is not fixed until the redox reactions are largely finished. In particular, it is reasonable to expect that the uncompensated moment associated with an interface may change in magnitude and direction while such reactions take place. It is conceivable, and consistent with the present data, that the structural and electronic evolution of the interface during these reactions is partly influenced by the magnetization of the FM layer, so that a particular bias direction can be more easily accommodated. The data suggests that for the development of a biased state during the latent-period, it may be unnecessary for the AFM-FM couple to pass through a temperature region in which the magnetocrystalline anisotropy and/or the exchange energy of the AFM are low enough for the polarized FM to impose an optimum distribution of the orientations of the interfacial AFM crystallites' Néel axes, and, hence, the accompanying uncompensated spins (e.g., Refs. 1–3).

As an alternative, or in addition to these interfacial redox effects, there may be purely magnetic relaxation effects that can account for much of the observed behavior. In view of the polycrystalline nature of the films, and considering various competing interactions between grains within each film as well as across the interface, the as-deposited state is undoubtedly a frustrated, highly degenerate magnetic state. Hence, there is the potential for slow relaxation of the state in response to various experimental treatments. This can, in principle, account for the ability to bias an initially unbiased sample, as in experiments denoted “c-1” above. This relaxation can be thermally activated, or activated by non-equilibrium excitations resulting from the deposition process. Even a Co adatom with negligible kinetic energy will deliver 4.4 eV (condensation energy) to the substrate, and kinetic energies of sputtered atoms would likely be on the order of tens of eV. Each adatom would thus generate nonequilibrium phonons with a typical energy much higher than the room-temperature, thermal phonons. It is possible that such phonons could activate switching of AFM grains, although there is no specific theory for such nonthermal activation. However, the final experiments denoted “c-3” and “c-4,” that the bias can be reversed during the latent period after deposition, and that the bias cannot be reversed by taking an “aged” sample and depositing more SiO₂, seem to minimize the importance of such nonequilibrium effects during deposition.

To put this study in broader context, we note some recent findings with x-ray magnetic circular dichroism (XMCD) of interfacial magnetism in AFM-FM coupled films. In brief, the XMCD technique permits the identification of atom-specific interfacial net moments. XMCD studies in systems like ours, with monoxide AFM films, have shown reversible net moments on interfacial cations that were initially AFM.^{9,10} In fact, XMCD has shown that in our exchange

couples of Ni_{0.52}Co_{0.48}O—Co films, some Ni moments reverse as the field is cycled.¹¹ This implies a strong exchange interaction between some interfacial AFM Ni cations and adjacent FM Co atoms. Since these samples are in a biased state, these reversible AFM spins are presumably not directly responsible for exchange bias. The interfacial uncompensated spins, generally accepted to cause exchange bias, should be coupled more strongly to the core of the AFM film, and thus not reverse with the FM magnetization. As found in our earlier work,³ $H_E(T)$ shows the same qualitative behavior as that of the TRM of CoO/MgO multilayers, in which TRM is composed only of interfacial uncompensated spins. These moments are found to be insensitive to applied fields of the order of several Tesla. Furthermore, it is difficult on theoretical grounds to understand how moments that follow the FM magnetization during a hysteresis cycle can generate a fixed exchange bias. These reversible spins can be viewed as effectively part of the FM layer, and likely play a role in mediating the FM-AFM exchange interactions, but they do not play the central role of the interfacial uncompensated spins. Another issue to consider in the mediation of FM-AFM exchange is the potential for a proximity effect, similar to the induced moments in native oxides with an FeO structure on Fe.^{12,13} Here, a moment is induced in a layer having the structure of an antiferromagnet. Experimentally, this would be difficult to distinguish from the reversible AFM spins just discussed, which can arise in several ways, including interfacial reduction of the oxide or interdiffusion.

VII. CONCLUSIONS

For polycrystalline exchange-coupled films of Co on Ni_{0.52}Co_{0.48}O (50 nm), there is no difference in H_E and there is no training at RT, either when the couple is field-cooled through T_B , or when the Co film is deposited in a biasing field at temperatures well below T_B , providing that the Co film is ≥ 25 nm. As-deposited couples with thinner Co films show training, but the field-cooled ones do not. H_C exhibits no training for any of these samples. We found that the biasing field need be applied only during deposition of the first nm of a 25 nm Co film to produce the same H_E as when the biasing field was applied for the entire Co and SiO₂ capping layer deposition. In general, it was found that the biasing field need be applied only during a small initial or final portion of the Co deposition to establish the equilibrium H_E of a 25 nm Co film. This latter behavior, together with several more direct experiments, established the existence of a latent period, > 20 min, during which the direction of H_E could be completely or substantially reversed by reversing the biasing field. This latent period can plausibly be associated with the kinetics of the redox reactions, and with the relaxation of a highly frustrated magnetic state existing in the as-deposited condition. Finally, it was observed that the temperature dependence of H_E was qualitatively identical to that found for the uncompensated spins in CoO—MgO and CoO—SiO₂ multilayers. Our assumption that H_E is determined by the interfacial AFM uncompensated spins in this system is based

on that fact. Clearly, the validity of some of these suggestions requires more of the type of atom-specific interfacial data now becoming available from various types of spin probes.

ACKNOWLEDGMENTS

We are grateful to Fred Parker and Fred Spada for illuminating discussions on this work.

-
- ¹W. H. Meiklejohn and C. P. Bean, *Phys. Rev.* **102**, 1413 (1956).
²W. H. Meiklejohn and C. P. Bean, *Phys. Rev.* **105**, 904 (1957).
³Kentaro Takano, R. H. Kodama, A. E. Berkowitz, W. Cao, and G. Thomas, *Phys. Rev. Lett.* **79**, 1130 (1997).
⁴Dinesh Martien, Kentaro Takano, A. E. Berkowitz, and David J. Smith, *Appl. Phys. Lett.* **74**, 1314 (1999).
⁵H. C. Tong, C. Qian, L. Miloslavsky, S. Funada, X. Shi, F. Liu, and S. Dey, *J. Magn. Magn. Mater.* **209**, 56 (2000).
⁶D. Mauri, H. C. Siegmann, P. S. Bagus, and E. Kay, *J. Appl. Phys.* **62**, 3047 (1987).
⁷*Landolt-Börnstein*, New Series, III/27g (Springer-Verlag GmbH, Berlin, 1992), p. 30.
⁸S. Chikazumi, *Physics of Ferromagnetism*, 2nd ed. (Clarendon, Oxford, 1997), pp. 488–491.
⁹C. Sánchez-Hanke and C.-C. Kao, *J. Magn. Magn. Mater.* **226–230**, 1803 (2001).
¹⁰A. Scholl, M. Liberati, E. Arenholz, H. Ohldag, and J. Stöhr, *Phys. Rev. Lett.* **92**, 247201 (2004).
¹¹Eberhard Goering (unpublished).
¹²G. S. D. Beach, F. T. Parker, David J. Smith, P. A. Crozier, and A. E. Berkowitz, *Phys. Rev. Lett.* **91**, 267201 (2003).
¹³K. Mori, M. Yamazaki, T. Hiraki, H. Matsuyama, and K. Koike, *Phys. Rev. B* **72**, 014418 (2005).
¹⁴A. E. Berkowitz, Y. J. Tang, David J. Smith, and M. F. Hansen (unpublished).
¹⁵T. J. Regan, H. Ohldag, C. Stamm, F. Nolting, J. Lüning, J. Stöhr, and R. L. White, *Phys. Rev. B* **64**, 214422 (2001).
¹⁶O. Zaharko, P. M. Oppeneer, H. Grimmer, H. Horisberger, H.-Ch. Mertins, D. Abrahamson, F. Schäfers, A. Bill, and H.-B. Braun, *Phys. Rev. B* **66**, 134406 (2002).